Environmental Research Letters

LETTER

Changes in meandering of the Northern Hemisphere circulation

Giorgia Di Capua[1,2] and Dim Coumou[1]

[1] Potsdam Institute for Climate Impact Research, Earth System Analysis, D-14473 Potsdam, Germany
[2] University of Potsdam, D-14469 Potsdam, Germany

E-mail: dicapua@pik-potsdam.de

Keywords: Rossby waves, climate change, extreme events, mid-latitudes flow

Supplementary material for this article is available online

OPEN ACCESS

RECEIVED
17 March 2016

REVISED
23 August 2016

ACCEPTED FOR PUBLICATION
26 August 2016

PUBLISHED
22 September 2016

Abstract

Strong waves in the mid-latitude circulation have been linked to extreme surface weather and thus changes in waviness could have serious consequences for society. Several theories have been proposed which could alter waviness, including tropical sea surface temperature anomalies or rapid climate change in the Arctic. However, so far it remains unclear whether any changes in waviness have actually occurred. Here we propose a novel meandering index which captures the maximum waviness in geopotential height contours at any given day, using all information of the full spatial position of each contour. Data are analysed on different time scale (from daily to 11 day running means) and both on hemispheric and regional scales. Using quantile regressions, we analyse how seasonal distributions of this index have changed over 1979–2015. The most robust changes are detected for autumn which has seen a pronounced increase in strongly meandering patterns at the hemispheric level as well as over the Eurasian sector. In summer for both the hemisphere and the Eurasian sector, significant downward trends in meandering are detected on daily timescales which is consistent with the recently reported decrease in summer storm track activity. The American sector shows the strongest increase in meandering in the warm season: in particular for 11 day running mean data, indicating enhanced amplitudes of quasi-stationary waves. Our findings have implications for both the occurrence of recent cold spells and persistent heat waves in the mid-latitudes.

Introduction

Recent studies have shown that high-amplitude Rossby waves in the mid-latitude flow are statistically linked to weather extremes at the surface [1, 2]. Depending on geographical region, certain types of extreme weather are favoured during periods of strong wave amplitudes, including for example cold spells in eastern North America [2]. As an example, the recent 2013–2014 winter in the United States was characterised by several high-impact cold spells, which were associated with strongly meandering flow patterns (see figure 1).

Several mechanisms have been proposed which could affect Rossby wave characteristics. Classical studies have shown that anomalous sea surface temperatures in the tropical Pacific can generate quasi-stationary wave trains which can constructively interfere with and thereby alter the mid-latitude flow [3, 4]. Recent work by Trenberth *et al* shows that some of the observed mid-latitude circulation anomalies in recent years might have arisen from a negative phase of the Pacific Decadal Oscillation and associated tropical rainfall anomalies, reporting that the strongest changes occur in winter [5]. Others have stressed the importance of rapid warming in the Arctic, one of the most striking climate change signals observed today which is associated with a rapid decline in sea-ice and changes in snow cover [6–10]. These cryosphere changes might affect the flow in the mid-latitudes and both tropospheric [11] and stratospheric [6, 12, 13] mechanisms have been proposed. Also internal dynamical mechanisms could create high-amplitude, quasi-stationary Rossby waves [14, 15].

Irrespective of the underlying drivers, it is unclear whether Rossby wave characteristics have actually changed [7, 16–18]. Based on the minimum and maximum latitude of individual geopotential height

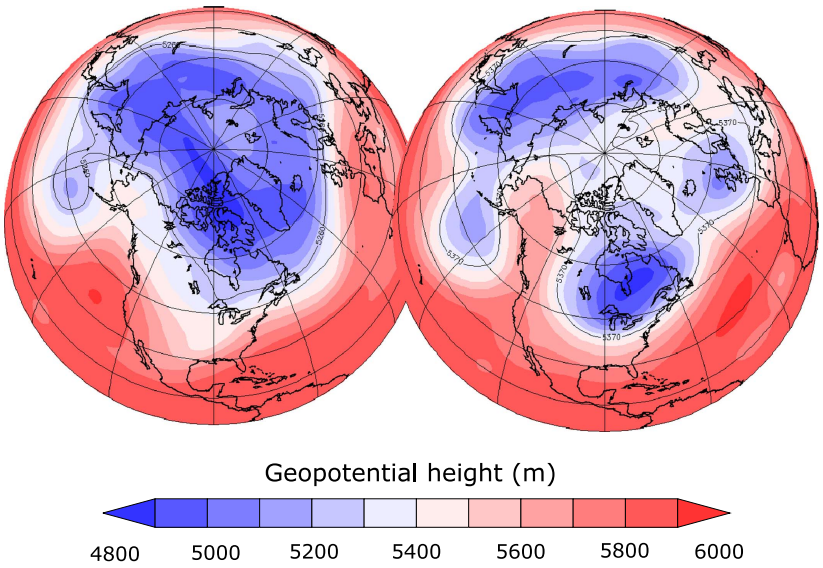

Figure 1. Geopotential height fields at 500 mb for (a) 5th of February 2011 and (b) 27th of January 2014. Solid black lines indicate the waviest isohypse with geopotential height (i) and meandering index (M) given in the panels. In panel (b) the anomalously low geopotential heights over north-east United States, related to the cold spell there, is clearly visible.

contours (or isohypses), Francis and Vavrus [7] claimed that peaks of ridges have moved northward and that the North–South extent of Rossby waves has increased over the North American sector. However, Barnes [19] demonstrated that these findings are sensitive to the methodology used and especially to the selected isohypse(s), showing that the claimed increase in latitudinal wave extent rather reflected an upward migration of maximum wave activity. Further studies have reported both little [17] and pronounced [18] changes but these analyses were again based upon selecting one or a limited set of isohypses and thus it remains unclear how robust their findings are. Thus, so far no clear evidence exists on whether mid-latitude circulation has become wavier or not over recent decades [6, 20, 21].

Here we introduce a new meandering index which measures the waviness of the middle troposphere based on the full shape of each isohypse. Moreover, the index accounts for possible migration of wave-activity by searching for maximum waviness at any given time (following Barnes). We present results for different regions and time scales. Our results show significant changes in the meandering of isohypses in different regions and running mean, adding evidence that changes in the waviness of the middle troposphere have occurred in the recent decades.

Meandering index

Figure 1 illustrates different meandering situations in the 500 mb geopotential height fields (Z500) over the Northern Hemisphere: figure 1(a) shows a typical zonally oriented flow pattern while figure 1(b) shows a strongly meandering one. The latter event occurred during the 2013–2014 winter, which saw several cold spells over the United States, as visible in the anomalously low geopotential heights over the northeastern US. The strongly meandering isohypse pattern simultaneously gave rise to extremely warm temperatures in California and Alaska [22].

We define a new, hemispheric meandering index '*M*' which is based upon the most strongly meandering isohypse in each individual day. This index accounts for the full path of the isohypse, without modifying or simplifying its shape, such that also shapes during wave breaking events (with multiple latitudinal positions of the isohypse at one longitude) are correctly considered.

The meandering index m of a single isohypse i is defined as:

$$m = \frac{\text{Arc length}(i,\ \theta_{\text{ref}})}{2\pi R\ \cos(\theta_{\text{ref}})}. \quad (1)$$

With Arc length(i, θ_{ref}) the arc length of the isohypse i, i.e. the walking-distance along isohypse i (see SI, figure S1), which is normalised to the Earth's circumference $2\pi R\cos(\theta_{\text{ref}})$ at reference latitude $\theta_{\text{ref}} = 60°$ (see Calculating arc length and normalising).

We calculate m for each isohypse in the range $Z = \{4900, 4905, 4910, \ldots, 6200\ \text{m}\}$ and define the combined meandering index M as the maximum of all m values:

$$M = \max_{i \in Z}(m) = \max_{i \in Z}\left(\frac{\text{Arc length}(i,\ \theta_{\text{ref}})}{2\pi R\ \cos(\theta_{\text{ref}})}\right). \quad (2)$$

This way, the waviest isohypse in Z500 is determined, as represented with solid black lines in figures 1(a), (b) and a large value is found for very wavy flow fields ($M = 2.4$ on 27/01/14). When a sub-region is considered, 2π is replaced by λ, where λ is the longitudinal distance of the sub-region in radians.

Calculating arc length and normalising

The aim of our index is to find maximum waviness in the atmosphere and therefore it should be able to compare meandering isohypses at different latitudes in a consistent way. In other words, we are only interested in the shape of an isohypse and its North–South deviations, but we want to make sure that its mean latitudinal position does not affect the value of our index. To do so, we map all isohypses to the same 2D grid centred around a common reference latitude $\theta_{\text{ref}} = 60\ ^\circ$N. The walking distance of the isohypse (or Arc length) is calculated within this 2D grid, which has a longitudinal extent of $2\pi\text{Rcos}(\theta_{\text{ref}})$, and thus the meandering index is normalised to the Earth's circumference at θ_{ref}. By normalising to one common reference latitude, we avoid that the same North–South deviation occurring in isohypses at different latitudes would result in different meandering indices. If one would normalise to the mean latitude of an isohypse (θ_{mean}) then a more northerly isohypse would have a higher index value than a southerly one if their shape (and thus North–South deviations) are the same. Nevertheless, we tested the influence of this effect and it turns out to be small: Our main findings are *not* sensitive to the exact choice of normalisation (i.e. to θ_{mean} instead of θ_{ref} or to other values for θ_{ref}). Both the significance and magnitude of the reported trends are quantitatively similar when a reference-latitude of 50° or 70° is used (see SI, figures S11–S18) or when the original latitude is used (see SI, figures S29–31). This choice makes the index independent of the latitude of the isohypse and also avoids that a poleward shift would increase the meandering index due to a change in mean latitudinal position and not by a real change in the shape of the isohypse. This way, any latitudinal migration of the waviest isohypse over time will not affect M but only changes in its shape will. We do however track the isohypse height and original mean latitude of maximum meandering (M) for further analysis (figure 5). The choice of $\theta_{\text{ref}} = 60°$ is justified as this is very close to the climatological mean latitude at which the waviest isohypses are found (see figure 5).

The arc length of i, i.e. the walking-distance along isohypse i, is determined in the 2D grid, giving the meandering index m of a single isohypse as defined in equation (1). This way, the index accurately differentiates between isohypses with strong North–South deviations from those which follow a circle of constant latitude, which is similar in rationale as other studies [17, 23, 24]. In spherical coordinates, northward deviations could actually have a similar or even shorter distance than the straight East–West distance due to the reduced circumference at higher latitude. We therefore do not calculate the arc length in spherical coordinates as the meandering index should capture deviations from the straight East–West direction. The isohypses have to circle the full hemisphere and thus local closed contours due to blocks or cut-off lows are excluded from the calculations. Next, we calculate m for each isohypse in the range $Z = \{4900, 4905, 4910, \ldots, 6200\ \text{m}\}$ and define the meandering index M as those m values which satisfy equation (2).

Data

We calculate M for daily 500 mb and 300 mb geopotential height fields from the ERA Interim [25] and the NCEP/NCAR [26] reanalyses for the period 1979–2015. Due to the higher spatial resolution of ERA Interim ($1.5° \times 1.5°$) compared to NCEP/NCAR ($2.5° \times 2.5°$) slightly larger meandering values are found for the former as meanders are measured to a finer scale. We calculate the meandering index both globally (i.e. around the hemisphere) and over the two continental sectors: the North American sector (180 °W–40 °W) and the Eurasian sector (40 °W–180 °E).

Next to daily data, 5 and 11 day running means are analysed. This way the influence of fast travelling free waves (i.e. the synoptic transients) and that of quasi-stationary waves can be separated. Synoptic transients have wave periods of 2–5 days [27] and thus will have a large influence when M is calculated on daily data but will be effectively filtered out when using 11 day running-means. Changes in the latter will thus reflect changes in quasi-stationary type waves.

For each of the three regions (global, America and Eurasia) and for all timescales, we statistically analyse the meandering index using quantile regressions to quantify changes in the full distribution of M rather than just changes in the mean. Any changes in upper quantiles (i.e. strongly meandering patterns) are particularly relevant as those have been linked to extreme weather [2]. Statistical significance of trends at $\alpha = 5\%$ is estimated using Monte Carlo analysis using 10 000 surrogate time series of shuffled data [28–30]. The shuffling algorithm accounts for the fact that running means present not truly independent data: Instead of considering 90 individual time series (one for each day of the season) with 37 values (one for each year) as done for daily data and perform shuffling of these series in time, when shuffling is applied on running means, blocks of 5 and 11 days (according to the respective running-mean) are shuffled.

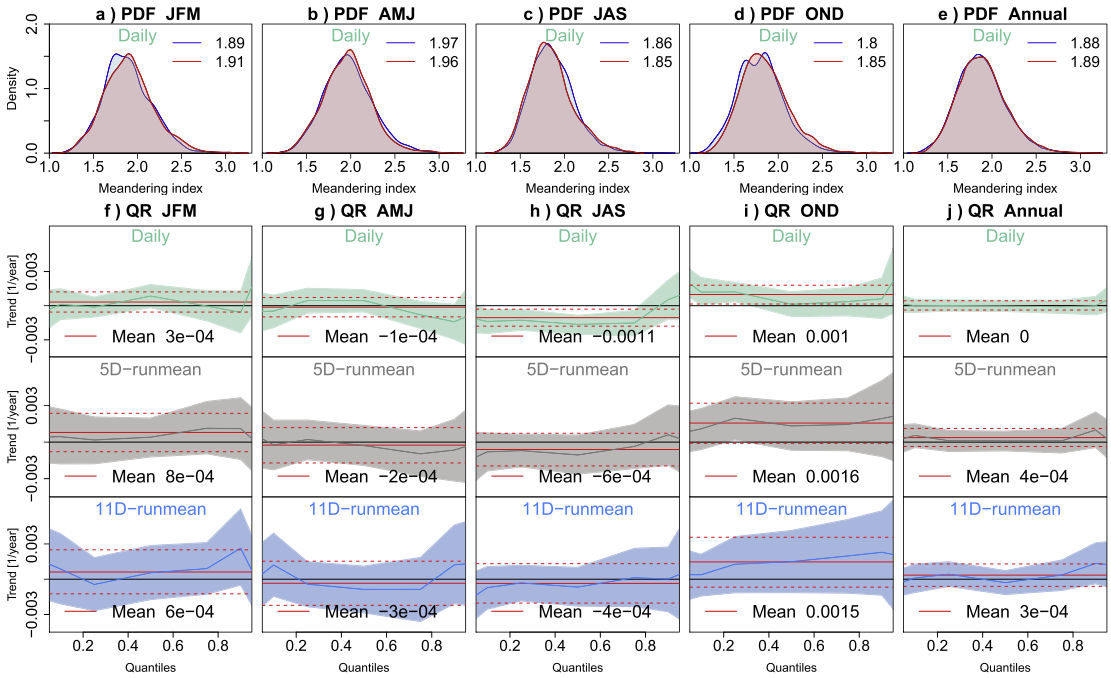

Figure 2. Top panels: probability density distributions of hemispheric meandering index (M) for 1979–1999 (blue) and 2000–2015 (red) for (a) winter, (b) spring, (c) summer and (d) autumn and (e) annual data based upon the Z500 ERA-interim reanalysis [25]. Mean values for each period are reported in the top-right corner. Bottom panels: associated trends in the mean (red solid line, with dashed red lines giving the 95% confidence interval) and in different quantiles (green for daily data, grey for 5 day running means, blue for 11-day running means and shaded regions giving the 95% confidence interval) for (f) winter, (g) spring, (h) summer, (i) autumn and (j) annual. Equivalent figure based upon NCEP-NCAR [26] figure S3. Equivalent figure based upon 300 mb geopotential height: figure S7.

Meandering index and arctic oscillation (AO) index

Strongly meandering flows (i.e. large M) are expected to be linked to a negative Arctic Oscillation (AO) index, which is confirmed by cross-correlation analyses (see SI, figures S33–S35). The correlation has a peak of significant negative values near lag 0 for the warm seasons in all running means, while in the cold seasons the correlation has a peak of significant negative values near lag 5 for daily data and lag 0 for the 11 day running mean. A negative correlation implies that when M increases, AO decreases, linking strongly meandering isohypses to negative AO situations as expected.

Hemispheric analyses

Figure 2 shows seasonal probability density distributions for daily data and quantile regressions for daily, 5 day and 11 day running means for the hemispheric meandering index M. A value $M = 1$ is the minimum theoretically possible value (representing a straight East–West isohypse) and the climatological mean is close to double that (1.9) for all seasons and for annual analysis (figures 2(a)–(e)). Next to the mean, also the shapes of the seasonal distributions are similar, reaching maximum values of $M \sim 3$.

For illustrative purposes, we compare the daily probability density distributions of M for two periods: 1979–1999 and 2000–2015. In autumn, the distribution has shifted to larger meandering values (figure 2(d)), consistent with a significant upward trend in the mean (figure 2(i), upper panel). Upward trends for both upper and lower quantiles reflect a shift of the distribution toward larger values with little changes in variance (although only trend for the 5th, 10th and 25th quantiles are significant). The trend in the mean of $\sim 10^{-3}\ \mathrm{yr}^{-1}$ is detected (and even larger) for 5 day and 11 day running means as well (figure 2(i), lower panels), but these are not significant because the confidence intervals become larger as less independent data are available. This persistence of the trends when synoptic waves are filtered out thus suggests that in autumn the increasing trend is mostly due to changes in quasi-stationary waves. Daily data in winter have seen no significant changes in M in neither mean nor quantiles (figure 2(f)).

In contrast to the cold seasons, daily M in summer shows a significant downward trend in the mean and in most quantiles. The observed trend in daily data ($-10^{-3}\ \mathrm{yr}^{-1}$) becomes smaller (and non-significant) in 5 day and 11 day running means (figure 2(h)) suggesting that the trends observed in daily data are mostly due to changes in synoptic wave activity, which is filtered out when using running means. Spring and

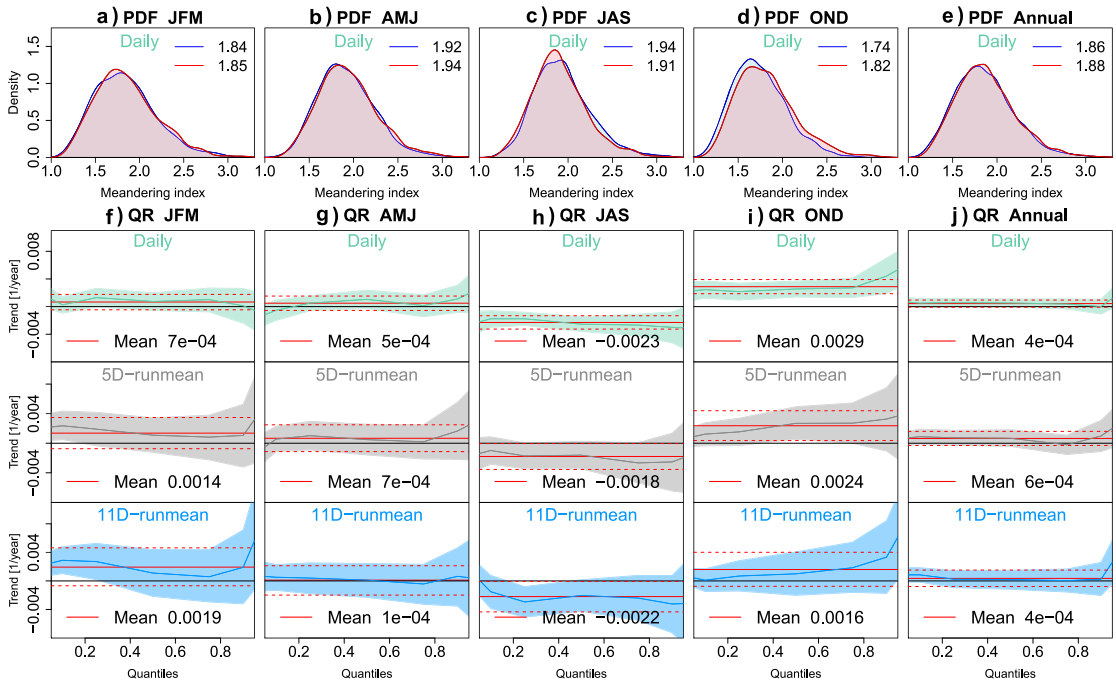

Figure 3. Top panels: probability density distributions of Eurasian meandering index (M) for 1979–1999 (blue) and 2000–2015 (red) for (a) winter, (b) spring, (c) summer and (d) autumn and (e) annual data based upon the Z500 ERA-interim reanalysis [25]. Mean values for each period are reported in the top-right corner. Bottom panels: associated trends in the mean (red solid line, with dashed red lines giving the 95% confidence interval) and in different quantiles (green for daily data, grey for 5 day running means, blue for 11 day running means and shaded regions giving the 95% confidence interval) for (f) winter, (g) spring, (h) summer, (i) autumn and (j) annual. Equivalent figure based upon NCEP-NCAR [26]: figure S4. Equivalent figure based upon 300 mb geopotential height: figure S9.

annual data have seen no significant changes in M at any timescale.

Regional analyses

Regional trends, as presented in figures 3 and 4, can typically be a factor 2 to 3 larger than those observed for the full hemisphere. The Eurasian sector (figure 3) is found to be dominant in determining the behaviour of the hemispheric index. The daily mean values are close to hemispheric ones (∼1.9), but the distribution is slightly broader with maximum values of $M \sim 3.3$ (figures 3(a)–(e)). Comparing distributions of the two periods, 1979–1999 and 2000–2015, the same tendencies as for the hemispheric index are found. Autumn shows a pronounced and significant upward trend in both the mean and all quantiles, with the stronger trend for the 95th quantile (0.005 yr^{-1}, figure 3(i), top panel). Similar to the hemispheric index, the trend in the mean (≈0.002 yr^{-1}) can be detected for daily, 5 day and 11 day running means, suggesting that changes in stationary wave activity are the most important contributors (figure 3(i)). Summer shows a significant downward trend in both mean (≈−0.0023 yr^{-1}) and most quantiles similar to the hemispheric index. Winter, spring and annual data show minor upward trends but none is significant.

Presented in figure 4, the American sector has seen different changes as compared to the hemispheric and Eurasian analyses. Though the climatological mean values are close to the hemispheric mean M values (∼1.9), the upper tail of the distribution stretches further with maximum values of $M \sim 3.5$. Autumn shows no significant changes neither in daily data nor in running-means. The warm seasons (AMJ-JAS) show generally upward trends with the largest magnitudes of trends observed in 11 day running means. This suggests that increased meandering of quasi-stationary waves has played the most important role in the warm seasons. In particular, in summer a non-significant upward trend appears in the 5 day running mean analysis, which becomes larger (0.003 yr^{-1}) and significant for 11 day running means (figure 4(h), lower panel). Both spring and summer 11-day running mean analyses show that the upper quantiles have seen the strongest trends, whereas the lower quantiles have seen essentially no trend, indicating a broadening of the distribution (figures 4(g)–(h), lower panels). Winter has seen no trend in the mean but a pronounced and significant upward trend (∼0.007 yr^{-1}) in the 95th quantile for daily data. The upward trends in high quantiles seen in most seasons can also be detected in the annual analysis showing significant increases in the 95th quantile for all time scales (figure 4(j)).

Figure 5 shows climatological mean values and linear trends for the seasonal and annual mean height and latitude where M is detected, i.e. where maximum

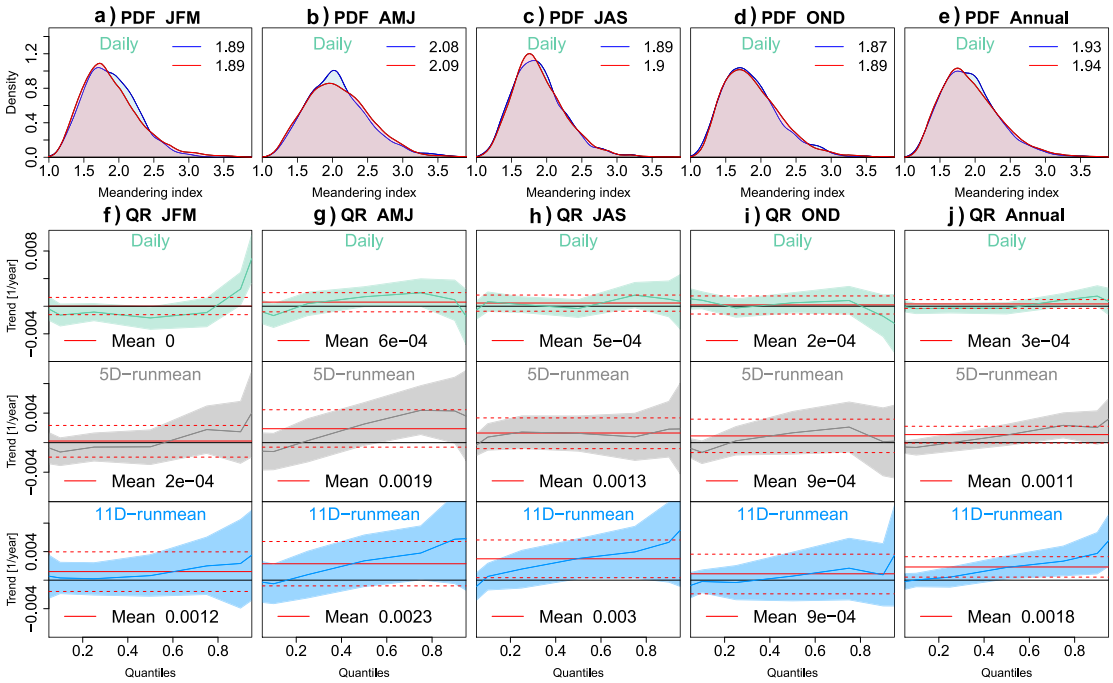

Figure 4. Top panels: Probability density distributions of American meandering index (M) for 1979–1999 (blue) and 2000–2015 (red) for (a) winter, (b) spring, (c) summer and (d) autumn and (e) annual data based upon the ERA-interim reanalysis [25]. Mean values for each period are reported in the top-right corner. Bottom panels: Associated trends in the mean (red solid line, with dashed red lines giving the 95% confidence interval) and in different quantiles (green for daily data, grey for 5 day running means, blue for 11 day running means and shaded regions giving the 95% confidence interval) for (f) winter, (g) spring, (h) summer, (i) autumn and (j) annual. Equivalent figure based upon NCEP-NCAR [26]: figure S5. Equivalent figure based upon 300 mb geopotential height: figure S8.

waviness occurs. In the hemispheric analysis, maximum waviness is usually found between 5200 and 5300 m in the cold seasons and between 5500 and 5600 m in the warm seasons (figure 5(a)). There are significant upward trends in this height by about 5–10 m/decade for all seasons and for annual data (figure 5(a)), indicating an upward migration of the waviest isohypse, likely reflecting warming of the lower troposphere. Mean latitudes are found between 60 °N and 62 °N, placing the waviest isohypse near the position of the climatological Polar jet (figure 5(d)). Autumn shows a significant poleward trend in the mean latitude of about 0.3°/decade. The other seasons and annual data show no trend in latitude (figure 5(d)).

Regionally, Eurasian maximum waviness tends to be at somewhat lower latitude and higher 500 mb geopotential heights, while in the American sector a slightly opposite tendency is found. However, values for both regions remain close to the hemispheric values. Note that for a specific day, maximum meandering in the different regions can occur at different isohypses, and hence different latitude and heights. Still only small differences are detected when the region is changed, as expected. At regional scale, a similar tendency of the most meandering isohypse to migrate toward higher heights is found, even though magnitude and significance of the trends can slightly change between different seasons and regions (figures 5(b) and (c)). In summer, the two regions show opposite behaviour in the latitudinal trends, with a significant southward trend in Eurasia and a significant but northward trend for the American sector. In autumn, Eurasia shows a significant northward trend, with the same tendency of the hemispheric latitudinal trend for this season. We repeated all our analyses using 300 hPa geopotential heights fields (SI, figures S7–S10) and for the NCEP/NCAR reanalysis (SI, figures S3–S6), which showed that our findings are robust.

Discussion

The meandering index *M* as defined here is different from indices defined previously like for example the DayMaxMin index [19], which captures the maximum North–South amplitude of isohypses but not their actual shape. These two indices therefore cannot be directly compared: the arc length of an isohypse can change even when its maximum North–South amplitude remains unaffected. The meandering index captures the total waviness in the atmosphere, which can be pronounced even when the North–South wave extent is moderate (i.e. when high wave numbers dominate). These two indices thus measure different aspects of the mid-latitude flow and therefore cannot be compared one-to-one. Other studies used spectral analysis to decompose isohypse patterns into their

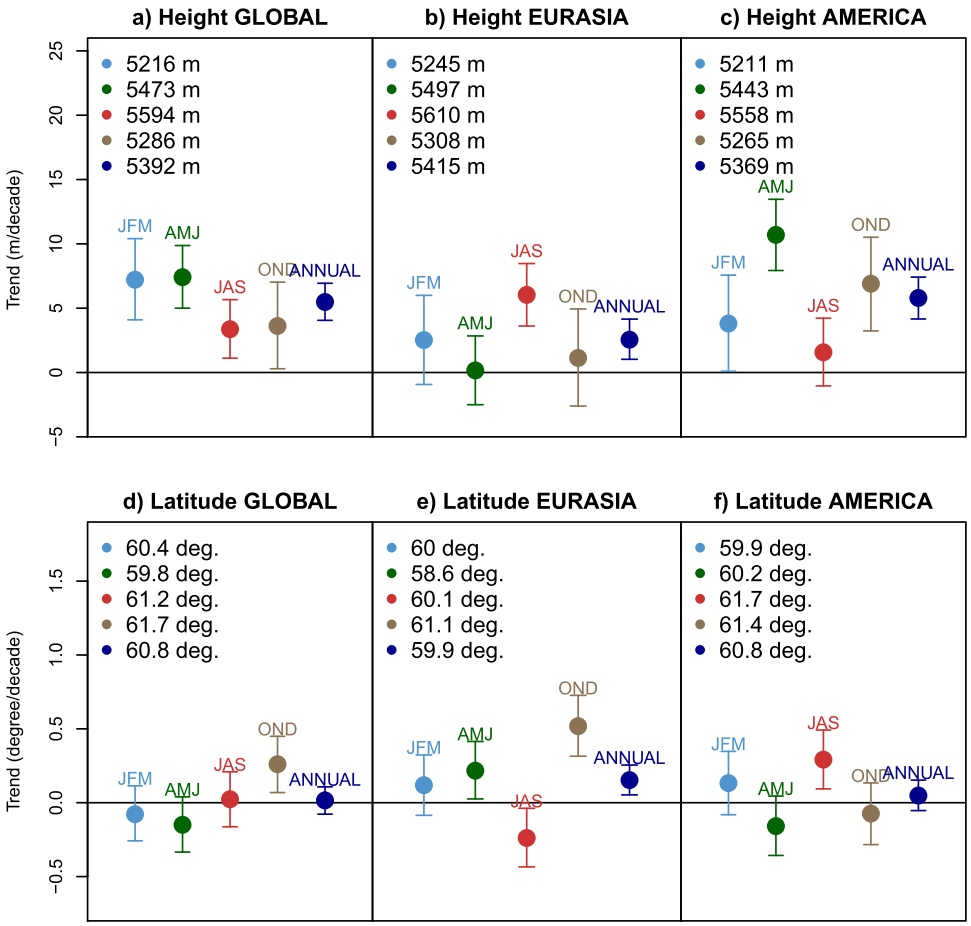

Figure 5. Top panels: trend in seasonal mean geopotential height for daily data where maximum meandering (*M*) is detected based upon the Z500 ERA-interim reanalysis [25] for (a) hemispheric, (b) Eurasian and (c) American sectors. Climatological mean values for the period 1979–2015 are reported in the top-left corners. Bottom panels: trend in seasonal mean latitude where maximum meandering (M) is detected based upon ERA-interim reanalysis [25] for (a) hemispheric, (b) Eurasian and (c) American sectors. Climatological mean values for the period 1979–2015 are reported in the top-left corners. Error bars represent the 95% confidence interval. Equivalent figures based upon ERA-interim reanalysis for 5 and 11 day running means: figures S27–28. Equivalent figure based upon NCEP-NCAR [26]: figure S6. Equivalent figure based upon 300 mb geopotential height: figure S10.

different wave number contributions and analysed changes in amplitude of these wave numbers [17]. Spectral methods cannot handle multiple latitudinal positions of an isohypse for a single longitude (i.e. during Rossby wave breaking events) and thus they cut isohypses short in such situations. While this approximation is unlikely to affect isohypses with small *M*, it could substantially modify the shape of isohypses that are curling over (for example during wave breaking), forcing them into a 'less wavy' shape. Our approach is different in that we measure total waviness rather than focus on individual wave numbers and our meandering definition also correctly retains and measures events that are curling over. This is important since we are particularly interested in such strongly meandering flow patterns. To differentiate between transient and quasi-stationary waves (the latter normally have lower wave-numbers) we apply running mean filtering.

More generally, following Barnes [19], we argue that quantifying changes in maximum waviness, rather than in some pre-selected isohypse(s), provides more stable and insightful results. Results of the latter are very sensitive to the chosen isohypse(s). Seasonal distributions and trends in *M* are very similar in the two reanalyses and at different pressure levels, whereas they can differ substantially when analysing single isohypses (figure S32). Our method also illustrates the usefulness of quantile regressions to estimate changes in the full distribution of circulation patterns. Forcing of the polar jet, irrespective of the nature of the forcing, is likely to favour only some type of circulation patterns but this might have little or no effect on the mean circulation [31]. Using quantile regressions, changes in the frequency of rare, strongly meandering patterns can be quantified.

We have reported significant trends in maximum waviness, with an overall tendency towards more strongly meandering circulation patterns. The detected trends appear to be rather moderate in magnitude, on the order of 0.1% yr^{-1} or about 4% change over 1979–2015, but they can nevertheless have pronounced effects on the occurrence-frequency of strongly meandering flow patterns. To illustrate this, we estimate the 90th percentile of *M* in 1979–1999 and

calculate how often this threshold is exceeded in 2000–2015. Autumn has seen significant upward trends in the hemispheric analysis (figure 2(i)) resulting in the 90th percentile ($M = 2.12$) to be exceeded in ~15% of autumn days in the post-2000 period, representing a ~50% increase compared to 1979–1999. Likewise, the Eurasian sector has seen a similar ~55% increase in meandering patterns exceeding the 90th percentile and even a ~74% increase of those exceeding the 95th percentile. The American sector has seen the strongest changes in summer for the 11 day running means, with an increase in events exceeding the 90th (95th) percentile of 50% (34%).

Our findings indicate that meandering in autumn-early winter (OND) has increased (significant trends in hemispheric and Eurasian analysis) and that this has led to an increase in occurrence-frequency of strongly meandering flow patterns. This might have favoured the occurrence of cold spells in recent autumns (though overall, cold seasons tend to become milder due to long-term warming trends). Drivers behind these autumn circulation changes are not analysed here, but previous studies have proposed anomalous tropical Pacific sea surface temperatures [5], anomalous extra-tropical sea-surface temperatures [32] or rapid warming in the Arctic [6]. Also internal atmospheric variability might well play a role [33, 34].

The warm season (JAS) has seen a more diverse behaviour among different seasons, regions and timescales. At the hemispheric scale, a significant downward trend is observed for daily data but this trend is not seen in 5 day or 11 day running means (figure 2(h)), suggesting that the observed daily trends are due to changes in synoptic wave activity. This is consistent with the recently reported hemispheric weakening of summer synoptic activity [35, 36, 37]. Weakening synoptic activity implies reduced synoptic pressure anomalies and hence the associated isohypse deviations from a straight line become smaller. Moreover, using spectral analysis of daily data of meridional wind fields, Coumou *et al* [35] show that, in summer, wave amplitudes have become smaller. The regional analysis shows that the Eurasian sector largely follows these hemispheric-wide changes but that the American sector has seen pronounced changes in the quasi-stationary wave. Here, we detect significant upward trends in the 11 day running mean data for JAS (and similar patterns for AMJ) indicating increased quasi-stationary wave amplitudes. This is particularly relevant for recent extreme weather events as the high quantiles have seen the most pronounced trends, as also detectable in the annual analysis (figures 4(g), (h), (j) lower panels). The drivers behind this enhanced meandering might include western north-Pacific sea-surface temperatures [38], changes in the Arctic cryosphere [39], or internal atmosphere-dynamical mechanisms [40, 41]. Irrespective of the underlying drivers, the tendency towards more-pronounced quasi-stationary meandering conditions during the American warm season might contribute to more-persistent weather and prolonged heat and drought conditions.

The aim of this study was to analyse maximum waviness in the Northern Hemisphere atmosphere via an index which is not affected by vertical or latitudinal migration of maximum waviness. We reported some robust and significant changes in this index which are relevant for mid-latitudes extremes associated with strongly meandering flow patterns. Future work should analyse possible drivers behind these changes.

Acknowledgments

We thank the anonymous reviewers for the helpful comments and suggestions during the review phase. We thank Dr Elisa Palazzi, the University of Turin and ISAC-CNR for supporting this project in its early stage. This work was supported by the German Federal Ministry of Education and Research (Grant number 01LN1304A).

References

[1] Coumou D, Petoukhov V, Rahmstorf S, Petri S and Schellnhuber H J 2014 Quasi-resonant circulation regimes and hemispheric synchronization of extreme weather in boreal summer *Proc. Natl Acad. Sci. USA* **111** 12331–6

[2] Screen J A and Simmonds I 2014 Amplified mid-latitude planetary waves favour particular regional weather extremes *Nat. Clim. Change* **4** 704–9

[3] Palmer T N and Mansfeld D A 1984 Response of 2 atmospheric general circulation models to sea-surface temperature anomalies in the tropical East and West Pacific *Nature* **310** 485

[4] Trenberth K E, Branstator G W, Karoly D, Kumar A, Lau N-C and Ropelewski C 1998 Progress during TOGA in understanding and modeling global teleconnections associated with tropical sea surface temperatures *J. Geophys. Res.* **103** 14291

[5] Trenberth K E, Fasullo J T, Branstator G and Phillips A S 2014 Seasonal aspects of the recent pause in surface warming *Nat. Clim. Change* **4** 911–6

[6] Cohen J *et al* 2014 Recent arctic amplification and extreme mid-latitude weather *Nat. Geosci.* **7** 627–37

[7] Francis J A and Vavrus S J 2012 Evidence linking arctic amplification to extreme weather in the mid-latitudes *Geophys. Res. Lett.* **39** L06801

[8] Cohen J, Jones J, Furtado J C and Tziperman E 2013 Warm arctic, cold continents *Oceanography* **26** 1–12

[9] Cohen J L, Furtado J C, Barlow M A, Alexeev V A and Cherry J E 2012 Arctic warming, increasing snow cover and widespread boreal winter cooling *Environ. Res. Lett.* **7** 014007

[10] Screen J A and Simmonds I 2010 The central role of diminishing sea ice in recent Arctic temperature amplification *Nature* **464** 1334–7

[11] Petoukhov V and Semenov V A 2010 A link between reduced Barents-Kara sea ice and cold winter extremes over northern continents *J. Geophys. Res. Atmos.* **115** 1–11

[12] Kim B-M, Son S-W, Min S-K, Jeong J-H, Kim S-J, Zhang X, Shim T and Yoon J-H 2014 Weakening of the stratospheric polar vortex by Arctic sea-ice loss *Nat. Commun.* **5** 4646

[13] Kretschmer M, Coumou D, Donges J F and Runge J 2016 Using causal effect networks to analyze different Arctic drivers of mid-latitude winter circulation *J. Clim.* **29** 4069–81

[14] Petoukhov V, Petri S, Rahmstorf S, Coumou D, Kornhuber K and JoachimSchellnhuber H 2016 The role of quasi-resonant planetary wave dynamics in recent boreal

spring-to-autumn extreme events *Proc. Natl Acad. Sci.* **113** 6862–7
[15] Stadtherr L, Coumou D, Petoukhov V, Petri S and Rahmstorf S 2016 Record balkan floods of 2014 linked to planetary wave resonance *Sci. Adv.* **2** e1501428
[16] Barnes E A, Dunn-sigouin E, Masato G and Woollings T 2014 Exploring recent trends in Northern Hemisphere blocking *Geoph. Res. Lett.* **2** 638–44
[17] Screen J A and Simmonds I 2013 Exploring links between Arctic amplification and mid-latitude weather *Geophys. Res. Lett.* **40** 959–64
[18] Francis J A and Vavrus S J 2015 Evidence for a wavier jet stream in response to rapid Arctic warming *Environ. Res. Lett.* **10** 14005
[19] Barnes E A 2013 Revisiting the evidence linking Arctic amplification to extreme weather in midlatitudes *Geophys. Res. Lett.* **40** 4734–9
[20] Walsh J E 2014 Intensified warming of the arctic: causes and impacts on middle latitudes *Glob. Planet. Change* **117** 52–63
[21] Kintisch E 2014 Into the maelstrom *Science* **344** 250–3
[22] Wang S Y, Hipps L, Gillies R R and Yoon J H 2014 Probable causes of the abnormal ridge accompanying the 2013–2014 California drought: ENSO precursor and anthropogenic warming footprint *Geophys. Res. Lett.* **41** 3220–6
[23] Rohli R V, Wrona K M and McHugh M J 2005 January northern hemisphere circumpolar vortex variability and its relationship with hemispheric temperature and regional teleconnections *Int. J. Climatol.* **25** 1421–36
[24] Wrona K M and Rohli R V 2007 Seasonality of the northern hemisphere circumpolar vortex *Int. J. Climatol.* **27** 697–713
[25] Dee D P *et al* 2011 The ERA-interim reanalysis: configuration and performance of the data assimilation system *Q. J. R. Meteorol. Soc.* **137** 553–97
[26] Kalnay E *et al* 1996 The NCEP/NCAR 40-year reanalysis project *Bull. Am. Meteorol. Soc.* **77** 437–71
[27] Lehmann J, Coumou D, Frieler K, Eliseev A V and Levermann A 2014 Future changes in extratropical storm tracks and baroclinicity under climate change *Environ. Res. Lett.* **9** 084002
[28] Pollard E, Lakhani K and Rothery P 1987 The detection of density-dependence from a series of annual censuses *Ecology* **68** 2046–55
[29] Schreiber T and Schmitz A 2000 Surrogate time series *Physica D* **142** 346–82
[30] Di Capua G 2014 Statistical Rossby waves analysis: amplitude and meandering indices *Master Thesis*
[31] Palmer T N 1998 Nonlinear dynamics and climate change: Rossby's legacy *Bull. Am. Meteorol. Soc.* **79** 1411–23
[32] Peings Y and Magnusdottir G 2014 Forcing of the wintertime atmospheric circulation by the multidecadal fluctuations of the North Atlantic ocean *Environ. Res. Lett.* **9** 034018
[33] Barnes E A and Screen J A 2015 The impact of Arctic warming on the midlatitude jet-stream: can it? has it? will it? *Wiley Interdiscip. Rev. Clim. Change* **6** 277–86
[34] Sun L, Perlwitz J and Hoerling M 2016 what caused the recent 'warm arctic, cold continents' trend pattern in winter temperatures? *Geophys. Res. Lett.* **43** 5345–52
[35] Coumou D, Lehmann J and Beckmann J 2015 The weakening summer circulation in the Northern Hemisphere mid-latitudes *Science* **348** 324–7
[36] Chang E K M, Ma C G, Zheng C and Yau A M W 2016 Observed and projected decrease in Northern Hemisphere extratropical cyclone activity in summer and its impacts on maximum temperature *Geophys. Res. Lett.* **43** 2200–8
[37] Lehmann J and Coumou D 2015 The influence of mid-latitude storm tracks on hot, cold, dry and wet extremes *Sci. Rep.* **5** 17491
[38] Wang S Y, Hipps L, Gillies R R and Yoon J H 2014 Probable causes of the abnormal ridge accompanying the 2013–2014 California drought: ENSO precursor and anthropogenic warming footprint *Geophys. Res. Lett.* **41** 3220–6
[39] Petrie R E, Shaffrey L C and Sutton R T 2015 Atmospheric response in summer linked to recent Arctic sea ice loss *Q. J. R. Meteorol. Soc.* **141** 2070–6
[40] Petoukhov V, Rahmstorf S, Petri S and Schellnhuber H J 2013 Quasiresonant amplification of planetary waves and recent Northern Hemisphere weather extremes *Proc. Natl. Acad. Sci. USA* **110** 5336–41
[41] Coumou D, Petoukhov V, Rahmstorf S, Petri S and Schellnhuber H J 2014 Quasi-resonant circulation regimes and hemispheric synchronization of extreme weather in boreal summer *Proc. Natl. Acad. Sci.* 1412797111 **111** 12331–6